Sampling and quality metric estimation of bimanual grasps for multifingered robotic hands

António Dinis
Department of Electrical Engineering
Instituto Superior Técnico, Universidade de Lisboa
Lisbon, Portugal
antonio.dinis@tecnico.ulisboa.pt

Plinio Moreno
LarSyS, Instituto de Sistemas e Robótica
Instituto Superior Técnico, Universidade de Lisboa
Lisbon, Portugal
plinio@isr.tecnico.ulisboa.pt

***Abstract*—We introduce a tool for sampling bimanual grasps with humanoid hands, as well as the study of quality metrics for bimanual grasps. The grasp sampler has three stages: (i) generating single hand grasps for left and right hand grasps, (ii) selecting pairs of right and left hand grasps to build bimanual grasps and, (iii) computing the bimanual grasp quality metrics. Our dataset includes 8363 humanoid bimanual grasps, using 48 objects from Shapenet. The dataset and the software is available online[1]**

I. Introduction

Work has already been done to create tools to generate data sets of grasps on objects, such as: bimanual grip dataset [1]. In addition, some heuristics have been proposed to sample bimanual grasps [2], and single-hand grasps [3]. However, but none of the tools/methods developed have bimanual grasps performed by humanoid hands for different types of hands.

In this work we introduce a tool for generating a dataset of bimanual grasps for humanoid hands, which has the potential of being applied to any pair of humanoid hands. Our method relies on the generation of grasps for each hand in a separate manner, then we develop a heuristic that joins pairs of single-hand grasps to build the bimanual ones. Finally, we compute a set of bimanual grasp quality metrics, which are essential for learning models that aim to evaluate grasps on new objects.

The evaluation of bimanual grasps is done using four metrics: (i) Shape Complementarity metric [3], which evaluates the similarity between the shape of the hand and the surface of the object. It is calculated for each hand individually and then summed to get the bimanual grasp evaluation. (ii) Force Closure metric [4], [5], which checks the ability of the grasp to resist external forces applied to the object. It is based on the normals of the contact points. (iii) Dexterity metric [1], which represents the ability of the grasp to manipulate the object. It is calculated using the singular values of the grasp matrix. (iv) Torque Optimization metric [1], which evaluates the force required to hold the object. It is based on the direction of the force applied by the hand. Our dataset includes over 8K humanoid bimanual grasps, using 48 objects from Shapenet[6].

This work was supported by LARSyS FCT funding (DOI: 10.54499/LA/P/0083/2020, 10.54499/UIDP/50009/2020, and 10.54499/UIDB/50009/2020), the H2020 FET-Open project Reconstructing the Past: Artificial Intelligence and Robotics Meet Cultural Heritage (RePAIR) under EU grant agreement 964854, and by the Lisbon Ellis Unit (LUMLIS)

[1]https://shorturl.at/rBhiv

II. Background and Related Work

A. Matrix representation of a two-hand grasp

A bimanual grasp is characterised by all their contact points [1], represented as follows:

$$P = \{(p_{r,1}, p_{r,...}, p_{r,m}, p_{l,1}, p_{l,...}, p_{l,n}) | p_{r,i}, p_{l,i} \in \mathbb{R}^3\}, \quad (1)$$

where $p_{r/l,i}$ represents the ith contact point of the left (l)/right (r) hand, and m/n, represents the number of right/left hand contact points. The Grasp matrix [7] of a two-handed grip can then be represented by

$$G = \left[G_{r,1}, G_{r,...}, G_{r,m}, G_{l,1}, G_{l,...}, G_{l,n}\right], \quad (2)$$

where,

$$G_{l/r,i} = \left[I_{3\times3}, (\lfloor p_{l/r,i} \rfloor_\times)^T\right]^T \quad (3)$$

and $\lfloor p_{l/r,i} \rfloor_\times$ is the antisymmetric matrix of $p_{l/r,i}$.

B. DA^2 Dataset: Dexterity-Aware Dual-Arm Grasping

The DA^2 Dataset [1] that inspired this work, is created using a heuristic for sampling bimanual antipodal grasps[8], [9], [10] and a grasp evaluation model with four metrics. It includes 9 million bimanual grips from 6000 objects, from the work [6]. Although the antipodal grasp selection is fast, it reduces by a large margin the available grips. To ensure a large number of grips, the space around the object is divided into blocks, generating grip poses in each block, followed by collision tests. Individual grips are randomly paired and evaluated based on: (i) force closure, (ii) the minimum singular value of matrix G, and (iii) the orientation of the major axis of the force ellipsoid relative to gravity. The Force Closure metric reflects the hand's ability to resist to external forces in any direction [4], [5]. We follow the approximation from [11]:

$$GG^T \geq \epsilon I_{6*6}\,, GF = 0\,, \quad (4a)$$

$$\|Gc\|_2 = \left\| -\frac{Gf_t}{\|f_n\|_2} \right\|_2 = \omega\,, \quad (4b)$$

where $f = f_t + f_n = [f_{l,1}^T, f_{l,2}^T, f_{r,1}^T, f_{r,2}^T] \in \mathbb{R}^{12}$, is the set of forces exerted by the robotic hands, where f_t

and f_n are the tangent and normal components, respectively. $c = [c_{l,1}^T, c_{l,2}^T, c_{r,1}^T, c_{r,2}^T]^T \in \mathbb{R}^{12}$ is the collective vector of all the friction cones. $G = [G_{l,1}, G_{l,2}, G_{r,1}, G_{r,2}]$, represents the matrix that characterises the grip (2). ω represents the angle between the axis of the friction cone and the applied force. This value can be used as a metric of grip stability, with low values indicating greater grip stability.

The second metric used is the minimum singular value (σ_{min}) of the matrix G, which is directly related to the grasp's ability to withstand external disturbances [12]. The higher the minimum singular value, the better the grip's performance.

The last metric considers the force that the end-effector needs to exert on the object. This is modeled by the Force Ellipsoide [13] that is computed from G. The major axis of the matrix indicates the direction in which the grasp resists to disturbances. The metric is given by the angle between the major axis of the ellipsoid and the gravity vector, θ_G.

The three metrics are normalised to the interval $[0, 1]$ and combined to obtain a final assessment as follows:

$$Q_{for}^k = 1 - \omega^k, Q_{dex}^k = \sigma_m^k / \max \sigma, Q_{tor}^k = cos\theta_G^k \,, \quad (5)$$

$$Q_{score}^k = \alpha Q_{for}^k + \beta Q_{dex}^k + \gamma Q_{tor}^k \,, \quad (6)$$

where k represents the kth grasp and $\alpha + \beta + \gamma = 1$.

Since we aim to generate bimanual grasps with multifingered hands, the antipodal sampling method does not work. However, we use the evaluation metrics to compute the grasp quality. In the following we describe previous works that develop heuristics for sampling multifingered grasps [3].

C. Geometric Approach for Grasping Unknown Objects with Multifingered Hands

Conventional grasp sampling algorithms require CAD models of both the objects and the robotic hand, such as GraspIt! [14], which relies on eigengrasps for pregrasp selection. More recent methods employ other heuristics that aim to generate more diverse grasps, such as differentiable force closure [15], DexGraspNet [16], MutiGripperGrasp Toolkit [17] and Energy-based heuristic [18]. To tackle the computational complexity, these methods either: (i) sample randomly points to perform collision tests, (ii) using convex approximation of objects, and (iii) using GraspIt as initialization. Our aim is to: (i) avoid the bias from GraspIt! initialization, (ii) have diverse grasps as well and (iii) compute fast collisions by using an approximation of the shape of the hand. The work of [3] follows these premises while simplifying the hand shape with a C-shaped cylinder (as illustrated in Fig. 1).

The grasp sampling heuristic starts by randomly selecting a point on the object's point cloud. A collision test is performed with various orientations and finger positions. The test checks for object points inside the C-Shape. The hand configuration with the most closed fingers is chosen, and the hand moves towards the object until collision. If the C-Shape covers over 1000 points, the grasp proceeds to the optimization phase, which aims to enhance the shape complementarity metric,

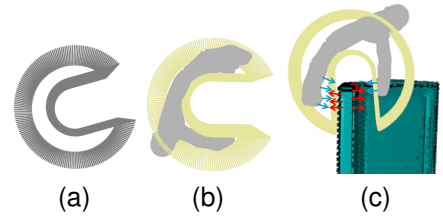

Fig. 1. (a) Wireframe representation of the C-Shape. (b) Overlay of the multifingered hand and its corrsponding C-Shape. (c) visual representation of the Shape Complementarity metric. The contact points of the hand and their normals are shown in blue and the contact points of the object and their normals are shown in red.

approximating the hand to a set of contact points. Each point is composed of its coordinate and associated normal, represented in blue in Figure 1(c). In this work we use the left and right RH8DR robotic hands[2].

The shape complementarity computes the distance between each contact point and the nearest point on the object, as well as the alignment between the respective normals:

$$e_p(\bar{c}_i) = r - \|\bar{c}_{p,i} - \pi_C(\bar{c}_i)\| \,, e_n(\bar{c}_i) = \langle -\bar{c}_{n,i}, n_c(\bar{c}_i) \rangle \,, \quad (7)$$

where $\pi_C(\bar{c}_i)$ is the Point Cloud point closest to the contact point $\bar{c}_i$ and is defined as

$$\pi_C(\bar{c}_i) = \underset{p \in C}{argmin} \|\bar{c}_{p,i} - p\|, s.t., \|\bar{c}_{p,i} - p\| \leq r, \quad (8)$$

where r is the maximum radius allowed to find the nearest point, $n_C(\bar{c}_i)$ is the normal associated with the nearest point and $\langle \cdot, \cdot \rangle$ is the scalar product. Finally, the Shape Complementarity metric is defined as

$$E_{shape}(s) = \frac{1}{M} \Sigma_{i=1}^{M_{nn}} e_p(\bar{c}_i) + w e_n(\bar{c}_i) \,, \quad (9)$$

where s represents the hand pose and joint configuration, M_{nn} is the number of contact points that have a closest point in the Point Cloud and w is a weight of the contribution of the normals to the final calculation of the metric.

The Particle Swarm Optimization algorithm [19] moves a set of possible solutions, called particles, around the search space of an optimization problem. Each particle's position represents the palm's pose and finger joint values. The algorithm iteratively adjusts the particles based on their best positions. It operates in two phases: first, adjusting the palm's position with fixed joint values, and second, optimizing the joint values while keeping the palm position fixed. This method is used to find single-hand grasps for left and right hands.

III. Bimanual grasp dataset generation

The method for creating the dataset consists of three stages: (i) Selection of individual grasps for the left hand and the right hand, (ii) finding pairs of left-right grasps, and (iii)

[2]https://www.seedrobotics.com/rh8d-adult-robot-hand

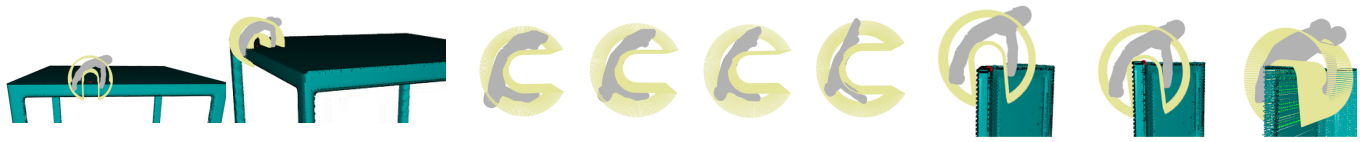

(a) Example of a two hand poses for the same same random point that collide with the C-shape.

(b) Each configuration of the C-shape is associated with a value for the angles of the finger joints. The values are chosen to use the full potential of the hand (using the maximum opening angle - 0 rad), but also representing the ability to perform grasps on small objects.

(c) On the left-hand side, the initial C-shape pose. In the middle, when the object is reached. All points that are inside the C-shape, i.e., the points that are between the two faces of the cylinder and have a radius smaller than the outer radius of the same, are saved.

Fig. 3. On the left, collision examples. On the middle, various C-shape configurations. On the right-hand side, object approach example

computation of the evaluation metrics for the bimanual grasps. We explain each stage in the following subsections.

A. One hand grasp sampling and selection

This heuristic includes searching for hand and finger poses that do not collide with the object, while simultaneously maximizing the number of points of the object involved and the similarity between the shape of the robotic hand and the surface of the object. The sequence of steps is as follows:

1) Random Point Selection: The selection of a random point on the object for each hand starts by dividing the object in two parts, one for left hand and the other for the right hand. Since the position of the object is aligned with the center of the robot's base, the object's reference frame was used to distinguish the points on the right side from the points on the left side. Fig. 2 illustrates the idea.

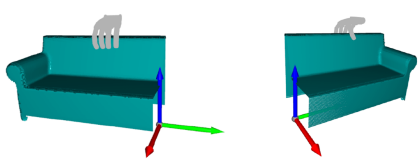

Fig. 2. Division of a couch into two parts. Left-hand side is used to sample randomly points for the left hand and right-hand side for the right hand.

2) Orientation Definition: The orientation of the grasp is then defined as the symmetric of the normal to the object at the selected point. Next, a collision test based on the C-shape is established between the hand and the object. If a collision is detected, a 45º rotation is applied to the C-shape around the normal to the object at the randomly chosen point, and a new collision test is performed. Up to three rotations are performed in the same direction. The images in figure 3a represent two examples of possible orientations taken by the C-Shape for the same random point, marked in red. Note that the collision with the object is detected in all orientations of the C-shape.

3) C-Shape parameter adjustment: If collisions are detected for all four orientations of the C-shape, its configuration is altered to represent a more open hand position. We follow [3], considering four different parametrizations of the C-shape, as illustrated in Fig. 3b.

4) Hand Movement: For each randomly chosen point, the C-shape with the smallest opening that does not cause collisions with the object is chosen and stored. Then, the robotic hand is moved in the opposite direction to the normal of the chosen point, approaching the object until it collides with the object. This procedure is illustrated in Fig. 3c.

5) Fingers pose optimization: The optimization process samples full hand poses with the Particle Swarm Optimization, which spread hand poses (i.e. particles) close to the current hand pose. If one of the particles improves the Shape Complementarity metric (9), the centroid of the particles is updated. The procedure is executed until collision occurs.

B. Constructing bimanual grasps

Each right hand grasp is associated with all the left hand grasps. The distance between the hands of each pair of hands is checked to see if there are collisions between them and if they are within the robot's range. The limits of the distance between the hands are set according to the size of the robotic hands and the robot's reach. More elaborated heuristics that consider other factors such as the orientation of the robotic hands were evaluated. However, these heuristics reduced highly the number of bimanual grasps. For this reason, only the distance between the hands factor was used.

C. Evaluation metrics

The contact points of the grasps are calculated during the optimization phase of the single-hand grasps, and are defined as the points on the object that lie inside the collision geometry of each link of the robotic hand at the moment the fingers are closing and reach the object. The contact points of both hands are joined into a single vector P, as expressed in (1), and its corresponding grasp Matrix G in (2). The four metrics are described as follows:

1) Shape Complementarity Bimanual: The Shape Complementarity metric is calculated for each of the hands individually in (9), and bimanual version is:

$$E_{\text{bimanual}} = E_{shape}(s_R) + E_{shape}(s_L), \tag{10}$$

where $E_{shape}(s_{R/L})$ is obtained from (9).

2) Force Closure: We follow the Force Closure approximation by [11] and applied in the work [1]. (4a) and (4b) replace the use of forces with the normals of the contact points. In our case, since there are lots of contact points, we normalize the Force Closure value of (4b) is then normalised so that the values are in the range $[0, 1]$:

$$\omega_b = 1 - \frac{||Gc||_2}{\max(||Gc||_2)}. \tag{11}$$

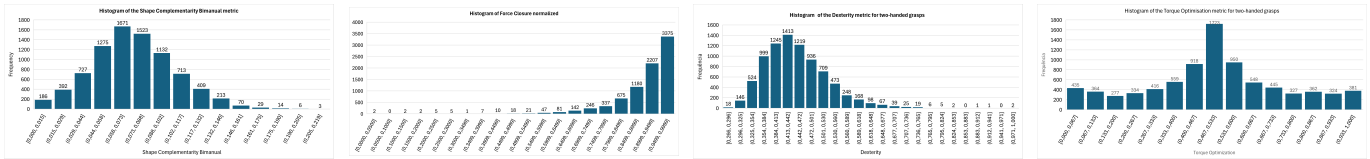

(a) Histograms associated with the Shape Complementarity bimanual metric. (b) Force Closure metric historgram for bimanual grasps. (c) Dexterity metric histogram for bimanual grasps. (d) Torque Optimisation metric histogram for bimanual grasps

Fig. 4. From left to right, histograms of Shape Complementarity, Force Closure, Dexterity and Torque Optimization.

3) Dexterity: This metric reflects the grasp's ability to exert force on the object in the weakest direction. This characteristic is obtained by decomposing the Grasp matrix, G, into minimum singular values by factorising it: $G = U\Sigma V^T$, where $U \in \mathbb{R}^{6\times6}$ and $V \in \mathbb{R}^{3N\times3N}$ are real orthogonal matrices and Σ is a diagonal matrix of size $6 \times 3N$ with the singular values of the matrix $\{\sigma_1, \sigma_2, ..., \sigma_m\}$. The Dexterity metric, d, is given by dividing the smallest singular value of the G matrix by the largest eigenvalue obtained:

$$d^k = \frac{\sigma^k_{\min}}{\max(\sigma)}, \tag{12}$$

where σ^k_{min} is the minimum eigenvalue relative to the handle k, and σ is the set of singular values of all objects.

4) Torque Optimization: This metric aims to assess how much force each grasp needs to apply, considering the gravity orientation. This indication is given by the angle between the gravity vector direction and the direction in which the bimanual grasp can exert the most force. This direction is obtained from the eigenvector of the GG^T matrix, which corresponds to the smallest eigenvalue. Since gravity takes the opposite direction of the z-axis, the cosine of the angle is given by dividing the y component by the z component of the selected eigenvector. The value is then transformed to ensure that it is in the range $[0, 1]$:

$$t = 0,5 + 0,5 \times \frac{v_z}{||v||}, \tag{13}$$

where v_y e v_z are the components of y and z, respectively, of the eigenvector corresponding to the smallest eigenvalue.

D. Recorded data

The recorded data includes: (i) Grasp information from Grasp matrix G, as well as the joint values for all the fingers of both hands, (ii) The four evaluation metrics; bimanual shape complementarity E_{bimanual} from (10), force closure ω_b from (11), dexterity from (12), and torque optimization t from (13), (iii) the valid contact points, P from (1) and their corresponding normals, and (iv) the object points enclosed by the C-shape after the swarm particle optimization. A dataset of bimanual grasps with 8,363 bimanual grasps and their evaluation metrics.

IV. Results

1) Shape Complementarity Bimanual: Figure 3a shows the histogram of the Bimanual Shape Complementarity metric (10), where the bins are in the $[0, 0.2]$ interval, approximately, and a higher frequency in the $[0.04, 0.1]$ interval. The shape of the histogram is similar to the single-hand grasps of [3].

2) Force Closure: Fig. 4b shows the distribution of results of the Force Closure metric, where it is observed that our results are in a much wider range than the range of values obtained in [1], which is restricted to the interval $[0, 1]$. We note that the increase in the Force Closure metric values is associated with the larger number of contact points and the shape of the robotic hand, since the Force Closure metric shows reduced values when the contact point normals have symmetrical orientations that cancel each other out.

3) Dexterity: The histogram shape and range of the bimanual dexterity are different from the ones obtained in [1]. In [1], the majority of values are higher than 0.8, but in our case vary mostly between 0.325 and 0.530, as can be seen in Figure 4c. The relationship between the dexterity metric values and the images of the bimanual grasps was also analyzed. However, it was not possible to establish a relationship between the dexterity values and the images of the bimanual grasps, in terms of the ability of the grasps to manipulate the object.

4) Torque Optimization: The Torque Optimisation metric takes values between 0 and 1, with a distribution illustrated in the Figure 4d. The histogram shape and range of values are similar to those of the [1], so our dataset has a good distribution for a learning model.

V. Conclusions

We present a new tool for generating bimanual grasps with multifingered hands. Our tool has three main blocks: (i) a heuristic for sampling individual grasps, (ii) creation of bimanual grasps, and (iii) bimanual grasp metrics computation.

The sampling process selects a set of individual grasp poses, checking the collisions with a simplyfied version of the hands. A set of bimanual grasps is created by combining the grasps sampled for the right hand with the grasps from the left hand. Finally, the bimanual grasps are evaluated according to four different evaluation metrics. On the one hand, of the metrics studied, it was concluded that Force Closure, Bimanual Shape Complementarity and Torque Optimisation are able to provide consistent values of the grasp quality, which can be used to train learning models that predict the quality of bimanual grasps. On the other hand, the Dexterity metric should not be considered yet, because the images of the grasps show that there is no explicit relationship between the quality of the grips and the value of the Dexterity metric.

REFERENCES

[1] G. Zhai, Y. Zheng, Z. Xu, X. Kong, Y. Liu, B. Busam, Y. Ren, N. Navab, and Z. Zhang, "Da^2 dataset: Toward dexterity-aware dual-arm grasping," *IEEE Robotics and Automation Letters*, vol. 7, no. 4, pp. 8941–8948, 2022.

[2] A. Rojas-de Silva and R. Suárez, "Grasping bulky objects with two anthropomorphic hands," in *2016 IEEE/RSJ International Conference on Intelligent Robots and Systems (IROS)*, 2016, pp. 877–884.

[3] M. Kiatos, S. Malassiotis, and I. Sarantopoulos, "A geometric approach for grasping unknown objects with multifingered hands," *IEEE Transactions on Robotics*, vol. 37, no. 3, pp. 735–746, 2020.

[4] S. P. Boyd and B. Wegbreit, "Fast computation of optimal contact forces," *IEEE Transactions on Robotics*, vol. 23, no. 6, pp. 1117–1132, 2007.

[5] T. Tsuji, K. Harada, and K. Kaneko, "Easy and fast evaluation of grasp stability by using ellipsoidal approximation of friction cone," in *2009 IEEE/RSJ International Conference on Intelligent Robots and Systems*. IEEE, 2009, pp. 1830–1837.

[6] M. Savva, A. X. Chang, and P. Hanrahan, "Semantically-enriched 3d models for common-sense knowledge," in *2015 IEEE Conference on Computer Vision and Pattern Recognition Workshops (CVPRW)*, 2015, pp. 24–31.

[7] D. Prattichizzo and M. Pozzi, "Robot grasp control," in *Encyclopedia of Systems and Control*. Springer, 2021, pp. 1885–1893.

[8] C. Eppner, A. Mousavian, and D. Fox, "ACRONYM: A large-scale grasp dataset based on simulation," in *2021 IEEE International Conference on Robotics and Automation (ICRA)*, 2021, pp. 6222–6227.

[9] ——, "A billion ways to grasps - an evaluation of grasp sampling schemes on a dense, physics-based grasp data set," in *Proceedings of the International Symposium on Robotics Research (ISRR)*, Hanoi, Vietnam, 2019.

[10] J. Mahler, J. Liang, S. Niyaz, M. Laskey, R. Doan, X. Liu, J. Aparicio, and K. Goldberg, "Dex-net 2.0: Deep learning to plan robust grasps with synthetic point clouds and analytic grasp metrics." Robotics: Science and Systems Foundation, 2017.

[11] T. Liu, Z. Liu, Z. Jiao, Y. Zhu, and S.-C. Zhu, "Synthesizing diverse and physically stable grasps with arbitrary hand structures using differentiable force closure estimator," *IEEE Robotics and Automation Letters*, vol. 7, no. 1, pp. 470–477, 2022.

[12] K. B. Shimoga, "Robot grasp synthesis algorithms: A survey," *The International Journal of Robotics Research*, vol. 15, no. 3, pp. 230–266, 1996.

[13] K. Shimoga, "Robot grasp synthesis algorithms: A survey," *The International Journal of Robotics Research*, vol. 15, no. 3, pp. 230–266, 1996.

[14] A. Miller and P. Allen, "Graspit! a versatile simulator for robotic grasping," *IEEE Robotics Automation Magazine*, vol. 11, no. 4, pp. 110–122, 2004.

[15] T. Liu, Z. Liu, Z. Jiao, Y. Zhu, and S.-C. Zhu, "Synthesizing diverse and physically stable grasps with arbitrary hand structures using differentiable force closure estimator," *IEEE Robotics and Automation Letters*, vol. 7, no. 1, pp. 470–477, 2021.

[16] R. Wang, J. Zhang, J. Chen, Y. Xu, P. Li, T. Liu, and H. Wang, "Dexgraspnet: A large-scale robotic dexterous grasp dataset for general objects based on simulation," in *2023 IEEE International Conference on Robotics and Automation (ICRA)*. IEEE, 2023, pp. 11 359–11 366.

[17] L. F. Casas, N. Khargonkar, B. Prabhakaran, and Y. Xiang, "Multigrippergrasp: A dataset for robotic grasping from parallel jaw grippers to dexterous hands," in *2024 IEEE/RSJ International Conference on Intelligent Robots and Systems (IROS)*. IEEE, 2024, pp. 2978–2984.

[18] Y. Shao and C. Xiao, "Bimanual grasp synthesis for dexterous robot hands," *IEEE Robotics and Automation Letters*, vol. 9, no. 12, pp. 11 377–11 384, 2024.

[19] J. Kennedy and R. Eberhart, "Particle swarm optimization," in *Proceedings of ICNN'95 - International Conference on Neural Networks*, vol. 4, 1995, pp. 1942–1948 vol.4.

SUPPLEMENTARY MATERIAL

We present the visualization of the bimanual grasps that provide a qualitative support of the metrics' values.

A. Evaluation metrics

1) Shape Complementarity Bimanual: The Bimanual Shape Complementarity metric, obtained from the sum of the results obtained for both hands, shows a distribution of values in the $[0, 0.2]$ interval, approximately, and a higher frequency in the $[0.04, 0.1]$ interval, as shown in the histogram of the image .

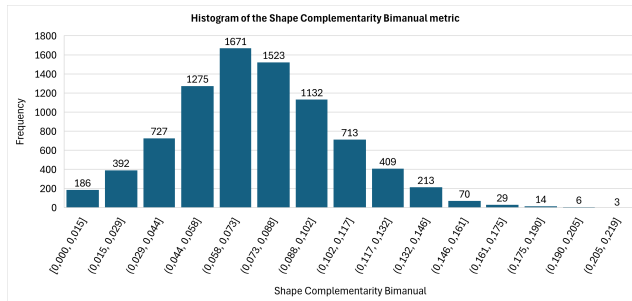

Fig. 5. Histograms associated with the Shape Complementarity bimanual metric

Looking at the images of some bimanual grasps with different Shape Complementarity values, you can see that the lower values correspond to low quality grasps, while the higher values correspond to better bimanual grasps. Figure 6 shows a set of two-handed grasps with a low Shape Complementarity value. Finally, the set of images in figure 7 shows a group of bimanual grasps with high Shape Complementarity.

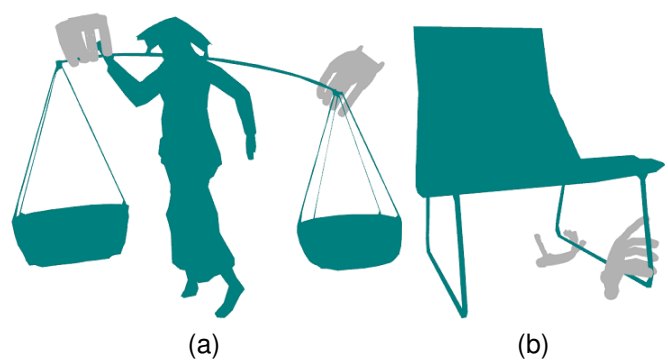

Fig. 6. Bimanual grasps with low Shape Complementarity, namely (a) 0.008 and (b) 0.013.

2) Force Closure: The results of the Force Closure metric include values between 0.6 and 4000 approximately, with a decreasing trend as the Force Closure value increases. Fig. 8 shows the distribution of results of the Force Closure metric.

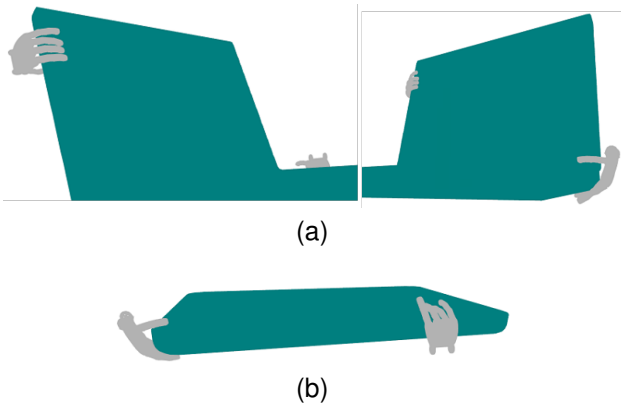

Fig. 7. Bimanual grasps with high Shape Complementarity, namely (a) 0.173 and (b) 0.197.

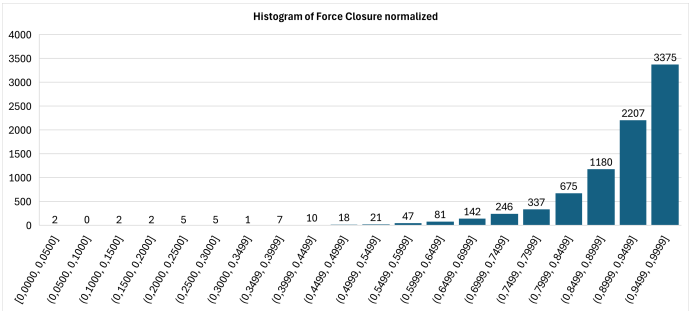

Fig. 8. Histogram associated with the Force Closure metric for two-handed grips.

It can be seen that the results obtained are in a much wider range than the range of values obtained in [1], which is restricted to the interval $[0, 1]$. From analysing the results, it was concluded that the increase in the Force Closure metric values is associated with the complexity introduced by the significant increase in the number of contact points and the shape of the robotic hand, since the Force Closure metric shows reduced values when the contact point normals have symmetrical orientations that cancel each other out.

Figure 9 shows a bimanual grasp with a Force Closure value of 0.58. From the set of images shown, you can see how the number of normals in one direction is similar to the number of normals in the opposite direction.

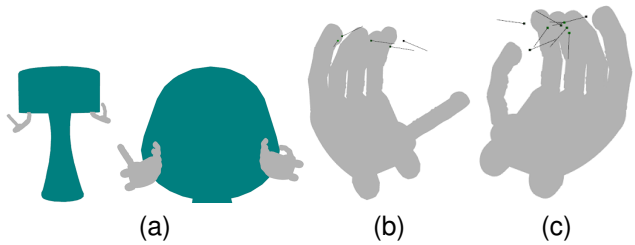

Fig. 9. (a) Example of a bimanual grasp with a Force Closure value of 0.58. Detailed view of the contact points of (b) the right hand and (c) the left hand.

In contrast to the grasps in the previous figures, in figure 10 we see a set of normals with a similar orientation. Therefore, the associated Force Closure value is high.

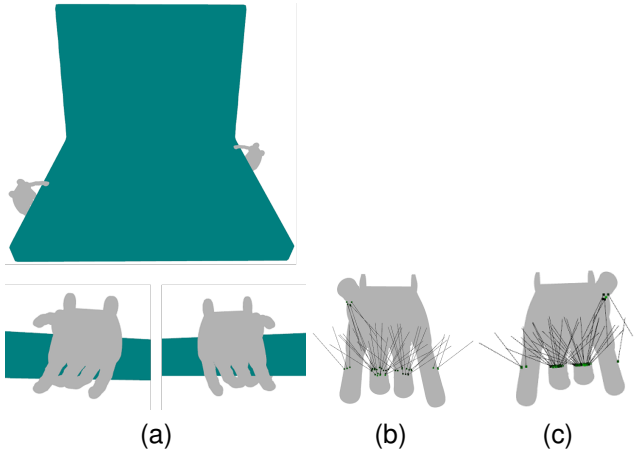

Fig. 10. (a) Representation of a bimanual grasp with a high Force Closure value of 2999. Detailed view of the contact points of (b) the right hand and (c) the left hand.

We can therefore see that calculating the Force Closure metric makes it possible to assess the ability of handles to resist forces from outside the object.

3) Dexterity: The results of the Dexterity metric for bimanual grasps show a different distribution of values to those obtained in [1] work. While in [1] show an upward trend, with the majority of values being higher than 0.8, in this work the values vary mostly between 0.325 and 0.530, as can be seen when analysing the histogram in Figure 11.

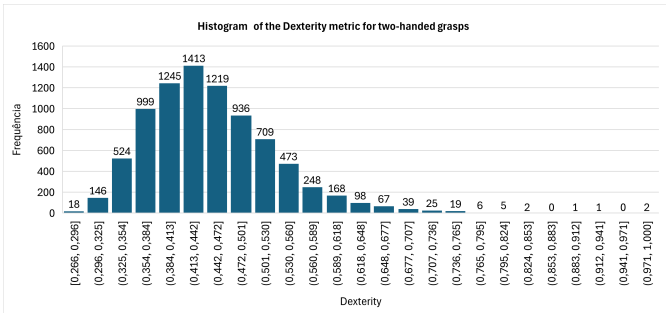

Fig. 11. Dexterity metric histogram for bimanual grasps

The relationship between the dexterity metric values and the images of the bimanual grasps was also analyzed. However, it was not possible to establish a relationship between the dexterity values and the images of the bimanual grasps, in terms of the ability of the handles to manipulate the object.

As an example, Figures 12a and 12b display two bimanual grasps with different Dexterity values, namely 0.1 and 0.370. Despite the difference in values, the distinction between each grip's ability to manipulate the object in all directions is unclear.

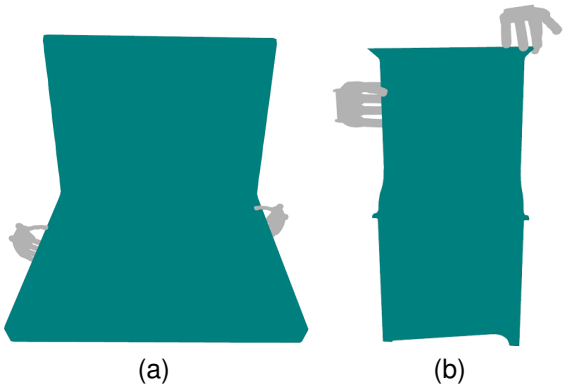

Fig. 12. Representation of a two bimanual grasps, with Dexterity values of (a) 0.1 and (b) 0.370.

4) Torque Optimization: The Torque Optimisation metric takes values between 0 and 1, with a distribution illustrated in the Figure 13.

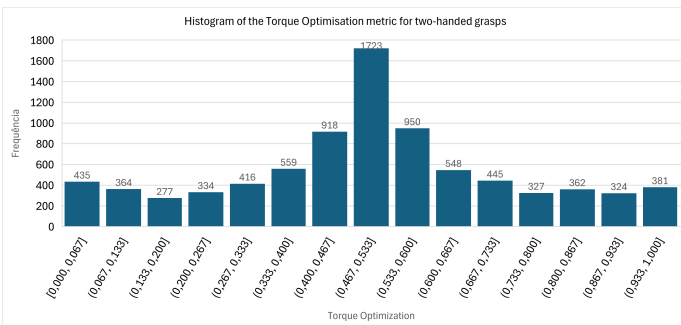

Fig. 13. Histograms associated with the Torque Optimisation metric for bimanual grasps.

The results obtained are similar to those of the [1] study in terms of the range of values covered and the distribution of values. In Figure 14 you can see a grasp whose Torque Optimisation metric value is 1 and the v vector has a direction similar to the positive direction of the z axis (blue).

On the other hand, the bimanual grasp shown in Figure 15 has a value for the Torque Optimisation metric of 0.003, and the v vector has a direction similar to the negative direction of the z axis (blue).

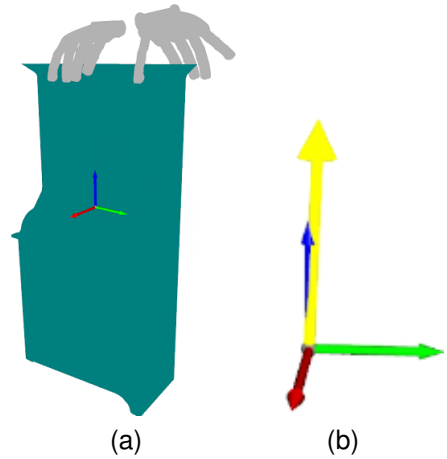

Fig. 14. (a) Representation of a bimanual grasp with a Torque Optimisation value of 1. (b) Representation of the vector showing the direction of the longest axis of the *Force Ellipsoid* in yellow.

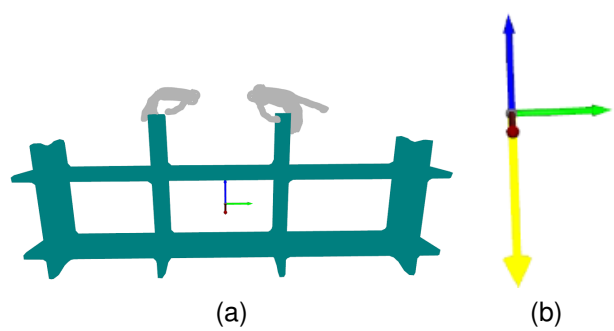

Fig. 15. (a) Representation of a bimanual grasp with a Torque Optimisation value of 0,003. (b) Representation of the vector showing the direction of the longest axis of the *Force Ellipsoid* in yellow.